Electronic Supplementary Information

Ultrathin Co_3O_4 Nanofilm as an Efficient Bifunctional Catalyst for Oxygen Evolution and Reduction Reaction in Rechargeable Zinc-Air Batteries

Yu He, Jinfeng Zhang, Guowei He, Xiaopeng Han*, Xuerong Zheng, Cheng Zhong, Wenbin Hu and Yida Deng*

Tianjin Key Laboratory of Composite and Functional Materials, Key Laboratory of Advanced Ceramics and Machining Technology (Ministry of Education), and School of Material Science and Engineering, Tianjin University, Tianjin 300072, China.

*E-mail: yida.deng@tju.edu.cn;

*E-mail: xphan@tju.edu.cn

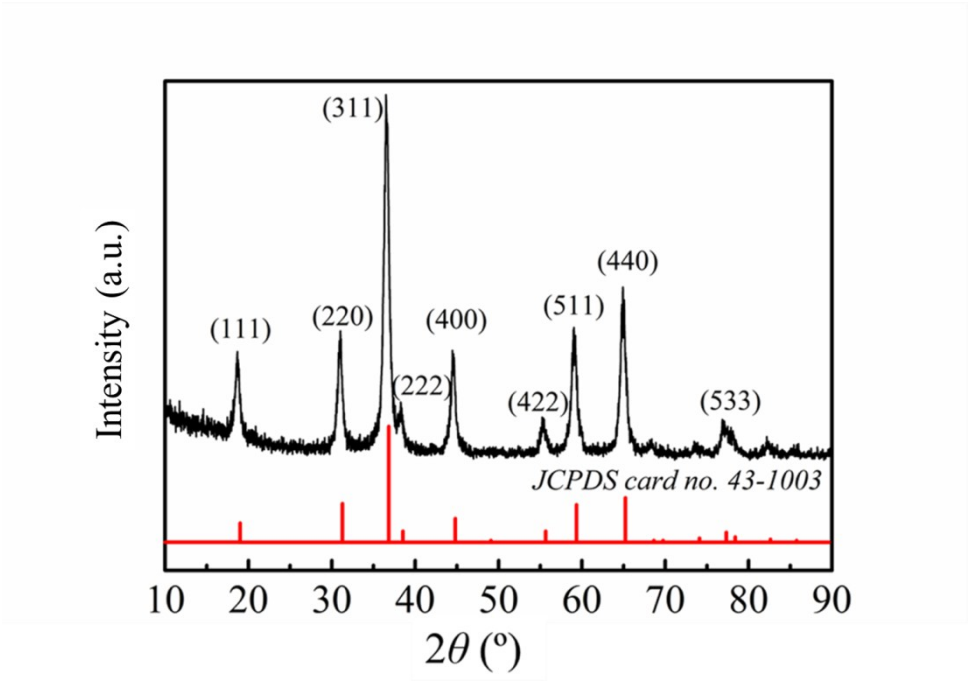

Fig. S1 XRD patterns of Co_3O_4 nanoparticle (black line) and standard PDF card of Co_3O_4 phase (red line).

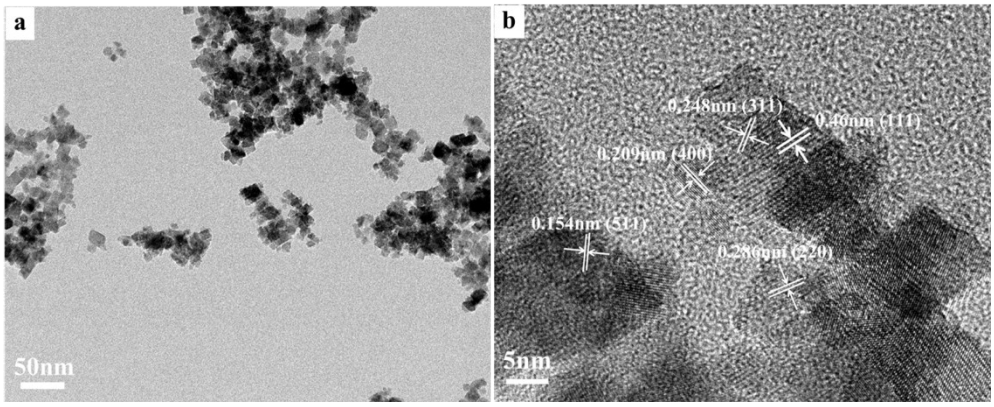

Fig. S2 TEM and HRTEM images of Co_3O_4 nanoparticle.

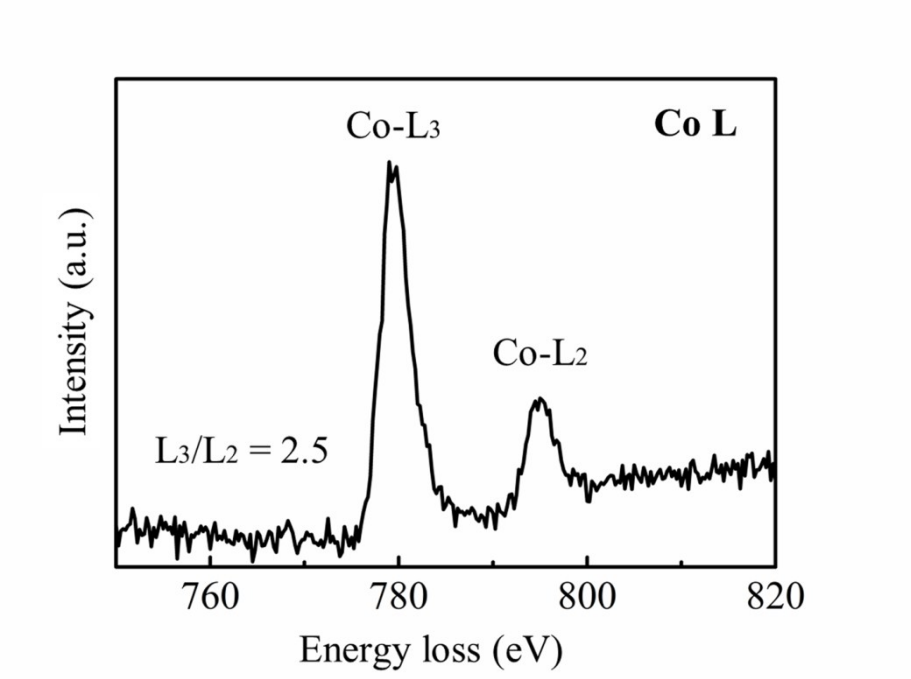

Fig. S3 Co $L_{2,3}$-edges electron energy loss spectrum of Co_3O_4 nanofilm.

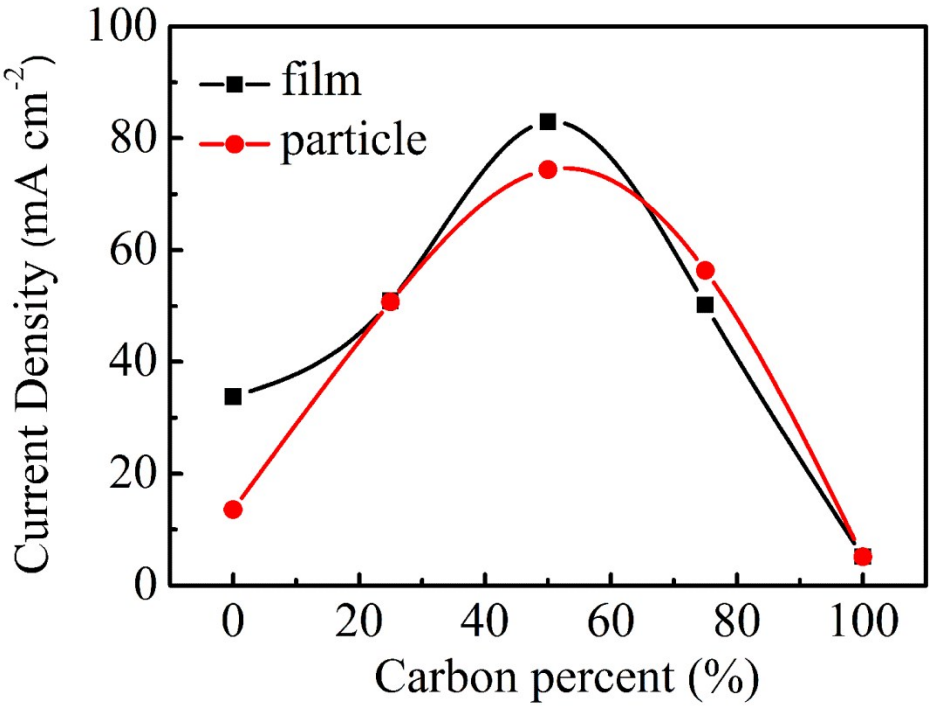

Fig. S4 The OER current density with different carbon proportion (0%, 25%, 50%, 75%, 100%) on glass carbon electrode at 1.87 V vs RHE.

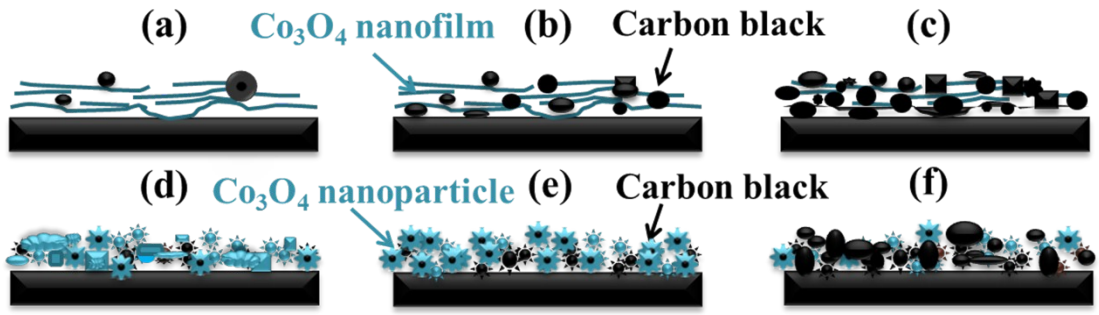

Fig. S5 The schematic diagrams (a, b and c) of Co_3O_4 nanofilm and (d, e and f) of Co_3O_4 nanoparticle with different amount of carbon additive. Lower percentage carbon added (a, d), moderate percentage carbon added (b, e), higher percentage carbon added (c, f). The blue area is nanofilm and the black represents conductive agent carbon particles.

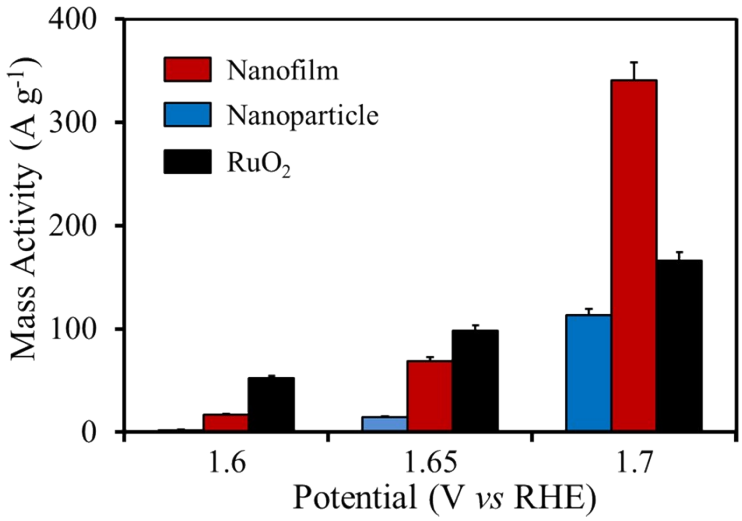

Fig. S6 Mass activity of corresponding samples at various potentials.

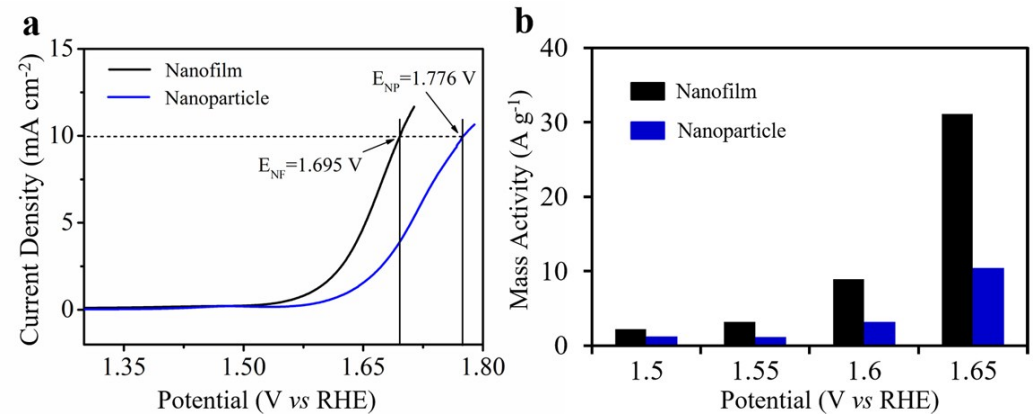

Fig. S7 (a) LSV polarization curves of Co_3O_4 nanofilm and nanoparticle loaded on GC measured in N_2-saturated 0.1 M KOH solution at a scan rate of 5 mV s^{-1} after iR correction. Catalyst loading was about 0.15 mg cm^{-2}. (b) Mass activity of corresponding samples at various potentials.

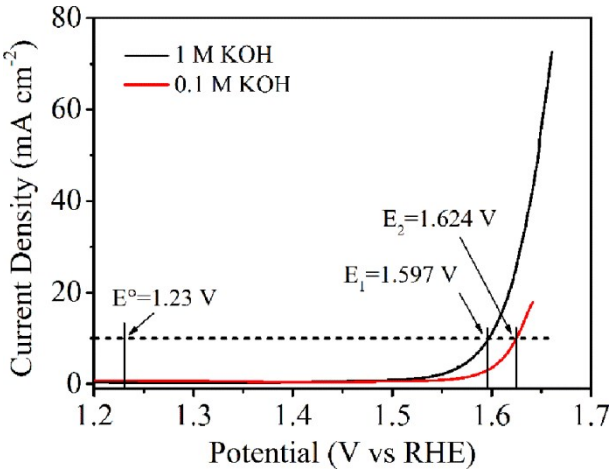

Fig. S8 (a) LSV polarization curves of Co_3O_4 nanofilm loaded on carbon fiber paper measured in N_2-saturated 1.0 M and 0.1 M KOH solution at a scan rate of 5 mV s^{-1} after iR correction. Catalyst loading is about 0.15 mg cm^{-2}.

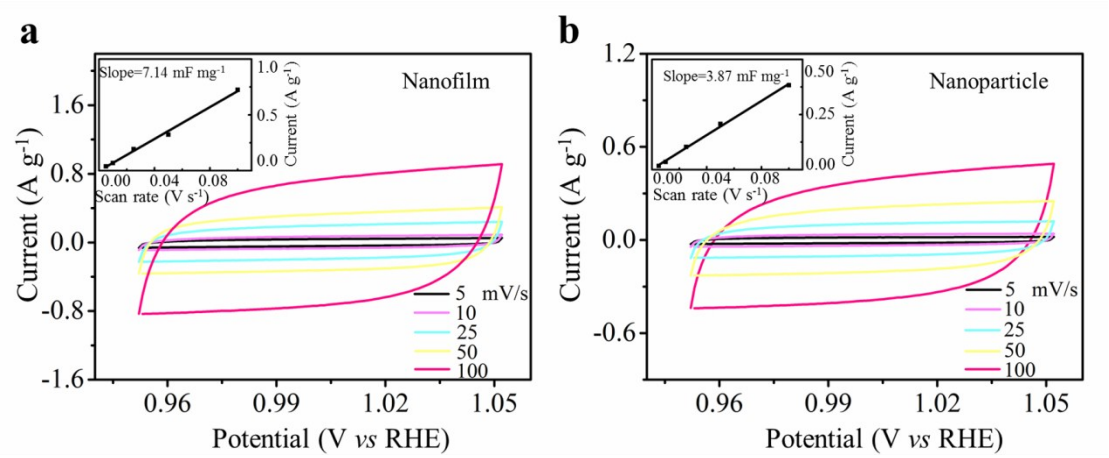

Fig. S9 Cycle voltammograms of (a) Co_3O_4 nanofilm and (b) Co_3O_4 nanoparticle from 0.95 to 1.05 V vs RHE at different scan rates in 0.1 M KOH and inset shows the corresponding linear fitting of the capacitive density versus scan rates.

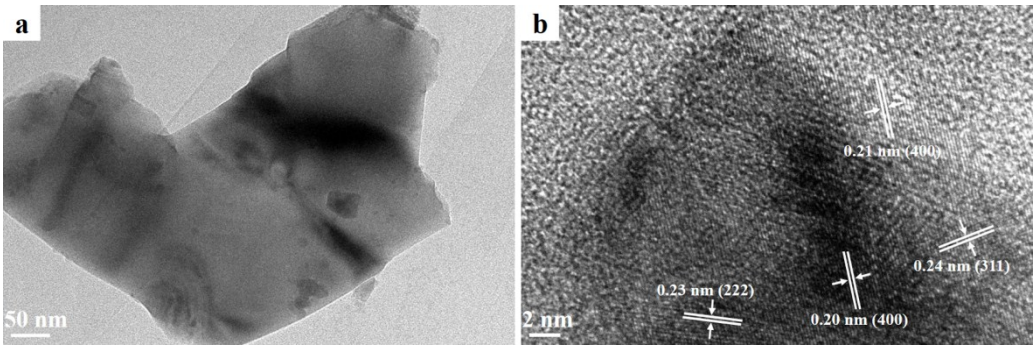

Fig. S10 TEM images of ultrathin Co_3O_4 nanofilm after long-time electrochemical stability test.

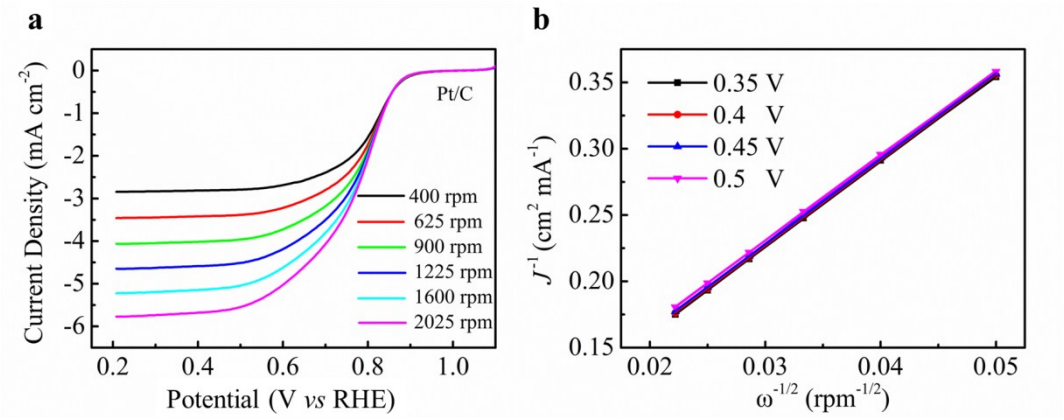

Fig. S11 (a) Rotating-disk voltammograms of Pt/C in O_2-saturated 0.1M KOH with a sweep rate of 5mV s^{-1} at various rotation rates. (b) K-L plots at different potentials.

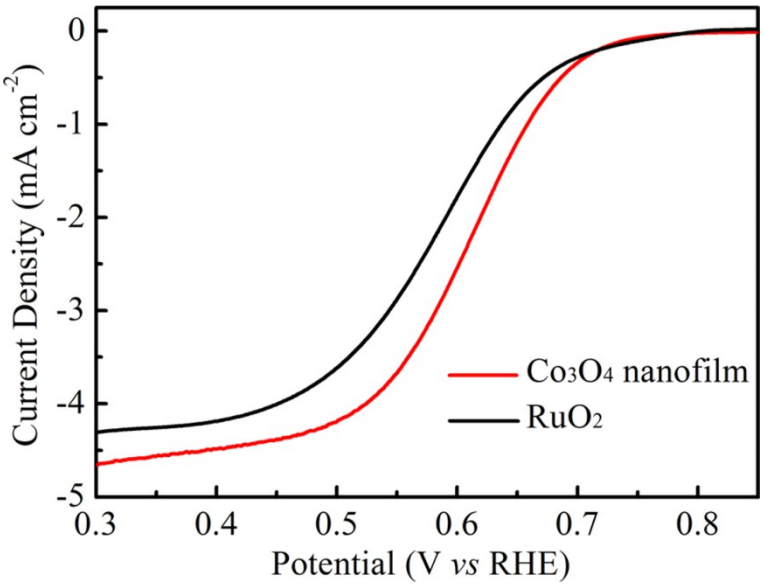

Fig. S12 (a) ORR activity of Co_3O_4 nanofilm and RuO_2 catalyst at 1600 rpm.

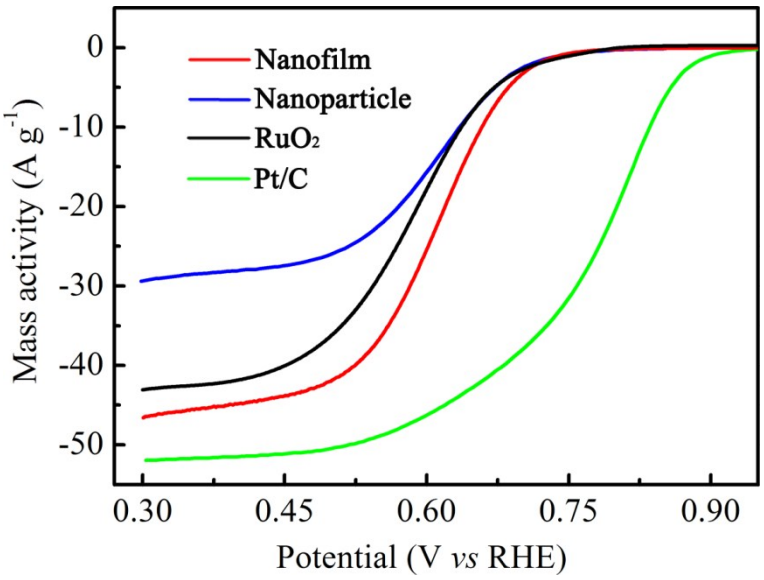

Fig. S13 Mass activities of Co_3O_4 nanofilm, Co_3O_4 nanoparticles, commercial RuO_2 and Pt/C catalyst on RDE at 1600 rpm in O_2-saturated 0.1 M KOH electrolyte. The loading is 0.1 mg cm^{-2} for all samples.

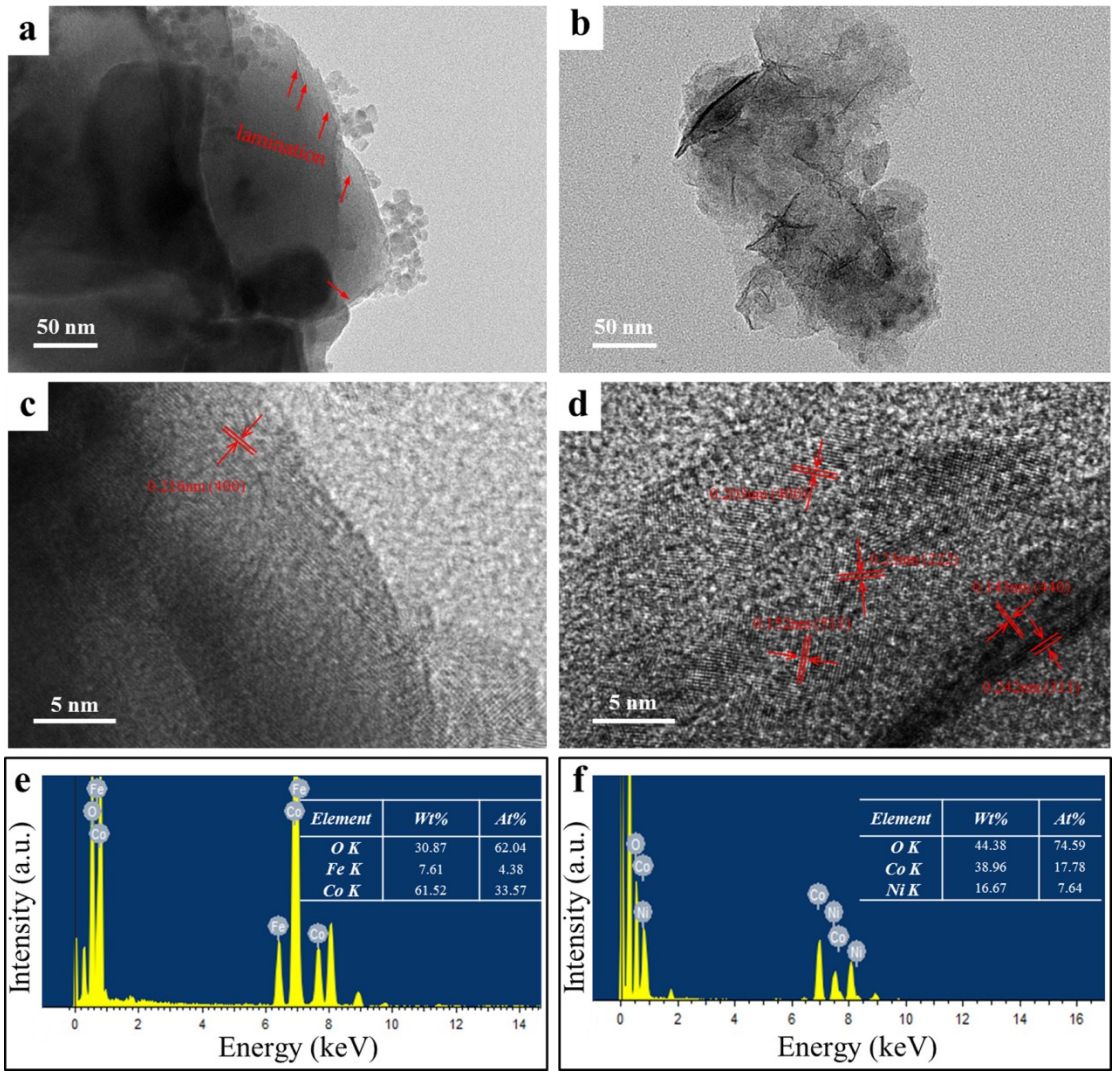

Fig. S14 (a, b) Low magnification, (c, d) high magnification TEM images and (e, f) EDS spectra of $Fe_xCo_{3-x}O_4$ (a, c, e) and $Ni_xCo_{3-x}O_4$ (b, d, f) nanosheet, respectively.

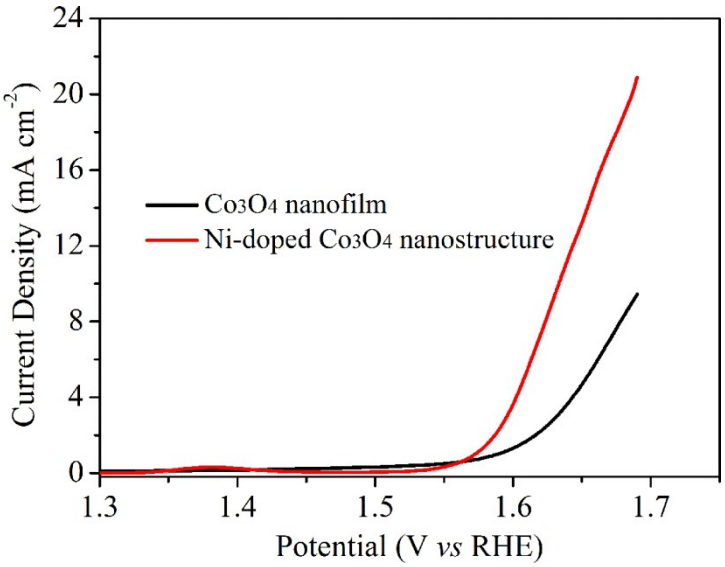

Fig. S15 OER performance of Co_3O_4 nanofilm and Ni-doped Co_3O_4 nanostructure in 0.1 M KOH solution.

Table S1. The analysis of the Co 2p and O 1s XPS spectra.

Catalyst	Co $2p_{3/2}$ (eV)	Co^{3+} peak and Area (%)	Co^{2+} peak and Area (%)	Co^{3+}/Co^{2+}	O_{lat} position (eV) and Area (%)	O_{ads} position (eV) and Area (%)	O_{ads}/O_{lat}
Co_3O_4 nanofilm	780.0	779.88 67.2	781.41 32.8	2.05	529.65 41.05	531.31 58.95	1.44
Co_3O_4 nanoparticle	780.2	779.75 64.6	781.25 35.4	1.82	529.64 47.94	530.77 52.06	1.08

Table S2. The electrocatalyticactivities of recently reported catalysts for OER in 0.1 M KOH.

Catalyst	Potential at 10 mA cm^{-2} (mV)	Electrolyte	Support	Mass activity (A g^{-1}) at 1.65 V	References
Co_3O_4 nanofilm	1.62	0.1 M KOH	CFP	137.5	this work
Co_3O_4 nanofilm	1.65	1.0 M KOH	GC	68.9	this work
Co_3O_4/Co_2MnO_4 nanocomposite	1.77	0.1 M KOH	GC	~22	S1
NiCo@NCNTs	1.64	0.1 M KOH	GC	~24	S2
CoO@Co/N-rGO	1.65	0.1 M KOH	GC	~51	S3
Zn-Co-S NS/CFP	1.62	1.0 M KOH	CFP	~107	S4
$Mn_3O_4@CoMn_2O_4$ $-Co_xO_yNPs$	1.68	0.1 M KOH	GC	~32	S5
Co-P film	1.57	1.0 M KOH	CFP	~46	S6
Co_3O_4@C-MWCNT (20 wt%)	1.61	1.0 M KOH	GC	~55	S7
$Ni_xCo_{3-x}O_4$ nanowire	1.6	1.0 M KOH	Ti foil	N.A.	S8
$La(Co_{0.71}Ni_{0.25})_{0.96}$ $O_{3-\delta}$	1.55	0.1 M KOH	GC	~42	S9
$LaNi_{0.99}O_{3-\delta}$	1.60	0.1 M KOH	GC	~19.5	S9
$Ni_{0.33}Co_{0.67}S_2$ nanowires	1.6	1.0 M KOH	Ti foam	~100	S10
1D-$Co_3V_2O_8$	1.58	0.1 M KOH	GC	N.A.	S11
Co_3O_4	1.67	0.1 M KOH	GC	~23.8	S11

References

S1. D. Wang, X. Chen, D. G. Evans and W. Yang, *Nanoscale*, 2013, **5**, 5312-5315.

S2. J. Yu, Y. Zhong, W. Zhou and Z. Shao, *J. Power Sources*, 2017, **338**, 26-33.

S3. X. Liu, J. Zang, L. Chen, L. Chen, X. Chen, P. Wu, S. Zhou and Y. Wang, *J. Mater. Chem. A*, 2017, **5**, 5865-5872.

S4. X. Wu, X. Han, X. Ma, W. Zhang, Y. Deng, C. Zhong and W. Hu, A*CS Appl. Mater. Interfaces*, 2017, DOI: 10.1021/acsami.6b16602.

S5. Z. Luo, E. Irtem, M. Ibáñez, R. Nafria, S. Martí-Sánchez, A. Genç, M. de la Mata, Y. Liu, D. Cadavid and J. Llorca, *ACS Appl. Mater. Interfaces*, 2016, **8**, 17435-17444.

S7. N. Jiang, B. You, M. Sheng and Y. Sun, *Angew. Chem., Int. Ed.*, 2015, **127**, 6349-6352.

S6. X. Li, Y. Fang, X. Lin, M. Tian, X. An, Y. Fu, R. Li, J. Jin and J. Ma, *J. Mater. Chem. A*, 2015, **3**, 17392-17402.

S8. Y. Li, P. Hasin and Y. Wu, *Adv. Mater.*, 2010, **22,** 1926-1929.

S9. A. Vignesh, M. Prabu and S. Shanmugam, *ACS Appl. Mater. Interfaces*, 2016, **8**, 6019-6031.

S10. Z. Peng, D. Jia, A. M. Al-Enizi, A. A. Elzatahry and G. Zheng, *Adv. Energy Mater.*, 2015, **5**, 1402031.

S11. S. Hyun, V. Ahilan, H. Kim and S. Shanmugam, *Electrochem. Commun.*, 2016, **63**, 44-47.